Poiseuille and thermal transpiration flows of a highly rarefied gas: over-concentration in the velocity distribution function

SHIGERU TAKATA and HITOSHI FUNAGANE

Journal of Fluid Mechanics / Volume 669 / February 2011, pp 242 - 259
DOI: 10.1017/S0022112010005021, Published online: 16 February 2011

J. Fluid Mech. (2011), *vol.* 669, *pp.* 242–259.
doi:10.1017/S0022112010005021

Poiseuille and thermal transpiration flows of a highly rarefied gas: over-concentration in the velocity distribution function

SHIGERU TAKATA[1,2]† AND HITOSHI FUNAGANE[1]

[1]Department of Mechanical Engineering and Science, Kyoto University, Kyoto 606-8501, Japan

[2]Advanced Research Institute of Fluid Science and Engineering, Kyoto University, Kyoto 606-8501, Japan

(Received 25 May 2010; revised 29 July 2010; accepted 23 September 2010)

Poiseuille and thermal transpiration flows of a highly rarefied gas are investigated on the basis of the linearized Boltzmann equation, with a special interest in the over-concentration of molecules on velocities parallel to the walls. An iterative approximation procedure with an explicit error estimate is presented, by which the structure of the over-concentration is clarified. A numerical computation on the basis of the procedure is performed for a hard-sphere molecular gas to construct a database that promptly gives the induced net mass flow for an arbitrary value of large Knudsen numbers. An asymptotic formula of the net mass flow is also presented for molecular models belonging to Grad's hard potential. Finally, the resemblance of the profiles between the heat flow of the Poiseuille flow and the flow velocity of the thermal transpiration is pointed out. The reason is also given.

Key words: kinetic theory, non-continuum effects, rarefied gas flow

1. Introduction

Poiseuille and thermal transpiration flows are among the most fundamental problems in rarefied gas dynamics or in microfluidics and have been investigated by many researchers. At the early stage of the modern rarefied gas dynamics, analyses were made by the use of arbitrary assumptions on the velocity distribution function, such as the variational and moment methods. Direct numerical computations were also carried out, first on the basis of the model equations, such as the Bhatnagar–Gross–Krook (BGK or Boltzmann–Krook–Welander) model (Bhatnagar, Gross & Krook 1954; Welander 1954), and then of the original Boltzmann equation. An exhaustive list of references is beyond the scope of the present paper. The reader is referred to, e.g., Cercignani (2006) and Sone (2007) and the references therein for the background and representative results. Some references rather directly related to the present work will be cited at proper occasions.

In the present paper we come back to the above classical problems, especially those in the two-dimensional channel, because there occurs an interesting phenomenon of the over-concentration of molecules on velocities parallel to the walls in the highly rarefied regime (see figures 3 and 6 in Ohwada, Sone & Aoki 1989). We shall focus

† Email address for correspondence: takata@aero.mbox.media.kyoto-u.ac.jp

on this issue and clarify its structure. We also propose a numerical method that handles the difficulty arising from this phenomenon. The method enables us to obtain the net mass flow through the channel in that regime accurately. For the linearized Boltzmann equation, an accurate deterministic numerical method was established in the late 1980s (Sone, Ohwada & Aoki 1989) for the intermediate rarefied regime, and there is a general asymptotic theory for the slightly rarefied regime (Sone 1969, 1991). Thus, the proposed method fills the last gap for preparing the database of net mass flow that covers the entire range of the Knudsen number Kn, i.e. from the continuum to the free molecular regime.

In the case of the two-dimensional channel, the flows in the highly rarefied regime have been studied analytically by Cercignani (1963) for the Poiseuille flow and by Niimi (1971) for the thermal transpiration on the basis of the BGK equation. They reported that the net mass flow grows logarithmically in Kn ($Kn \gg 1$) as Kn is increased. In the analyses, they used an advantageous property of the model equation that the basic equation and its boundary condition can be reduced to a set of integral equations for macroscopic quantities. The same reduction can be applied to more sophisticated model equations such as the ellipsoidal statistical model (Holway 1963, 1966; Andries *et al.* 2000) and the McCormack model for gas mixtures (McCormack 1973). It cannot, however, be applied to the original Boltzmann equation. As a result, analyses of the flows in the highly rarefied regime on the basis of the Boltzmann equation have not been carried out for a long time, though the logarithmic growth in Kn has been expected.

Recently, Chen *et al.* (2007) studied the thermal transpiration in the highly rarefied regime on the basis of the linearized Boltzmann equation for hard-sphere (HS) molecules and proved rigorously mathematically the logarithmic growth of the induced mass flow. They introduced a pointwise estimate of the velocity distribution function in addition to the norm estimates that are widely used in mathematical studies of the Boltzmann equation. The pointwise estimate plays a key role in the proof of logarithmic growth. In the present paper, motivated by their result, we construct an iterative approximation method and clarify the behaviour of the gas in the highly rarefied regime for both the Poiseuille flow and thermal transpiration problems. The method is rather ordinary, but we will ensure its convergence and estimate the order of error at each stage of iteration explicitly. Consequently, we will have a clear view of practical numerical analyses, by which the structure of the over-concentration will be clarified.

The paper is organized as follows. We start from the statement and formulation of the problems in § 2 and summarize the mathematical estimates by Chen *et al.* (2007) in § 3. Then in § 4.1 we present an iterative approximation procedure and show its convergence and explicit error estimates at each stage of iteration in the highly rarefied regime. In § 4.2, we clarify the structure of the over-concentration on the basis of § 4.1. In § 4.3, we present the actual numerical method to be adopted that is based on the procedure in § 4.1. Numerical results are shown in § 5. Finally in § 6 we present an asymptotic formula of the net mass flow through the channel for large Kn, which is available not only for HS molecules but also for any molecular model belonging to Grad's hard potential (Grad 1963). We will also point out that the profiles of the heat flow in Poiseuille flow and of the flow velocity in thermal transpiration agree well with each other in the highly rarefied regime. The reason is also given.

2. Problem and formulation

Consider a rarefied gas between two parallel resting plates located respectively at $X_1 = \pm D/2$ ($D > 0$), where X_i are the Cartesian coordinates. The two plates are

kept at the temperature $T_0(1+\beta_T X_2/D)$ (β_T is a constant), and a uniform pressure gradient is imposed on the gas in the direction of X_2; i.e. the pressure is given by $p_0(1+\beta_P X_2/D)$. (It can be shown that the pressure is independent of X_1.) We will investigate the behaviour of the gas under the following assumptions:

(i) The behaviour of the gas can be described by the Boltzmann equation for hard-sphere molecules with a common diameter σ and mass m. (The restriction to HS molecules will be relaxed later in § 6.1.)

(ii) The gas molecules are diffusely reflected on the surface of the plates.

(iii) $|\beta_T|, |\beta_P| \ll 1$, so that the equation and boundary condition can be linearized around the reference equilibrium state at rest with temperature T_0 and pressure p_0.

Usually, the above problem with $\beta_T = 0$ (the case that the plate temperature is uniform) is called the Poiseuille flow problem, while that with $\beta_P = 0$ (the case of no pressure gradient) is called the thermal transpiration problem. We call the gap between the plates occupied by the gas the (two-dimensional) channel. It is known that a flow is induced along the channel in both problems.

Let us denote the molecular velocity by $(2RT_0)^{1/2}\boldsymbol{\zeta}$ and the velocity distribution function by $\rho_0(2RT_0)^{-3/2}[1+\phi(\boldsymbol{x},\boldsymbol{\zeta})]E(|\boldsymbol{\zeta}|)$, where $\boldsymbol{x} = \boldsymbol{X}/D$, $E(t) = \pi^{-3/2}\exp(-t^2)$, $\rho_0 = p_0/RT_0$ and R is the specific gas constant. Then, the problem is described by the following boundary-value problem for ϕ:

$$\zeta_i \frac{\partial \phi}{\partial x_i} = -\frac{\nu}{k}\phi + \frac{1}{k}K(\phi), \tag{2.1}$$

$$\phi = (|\boldsymbol{\zeta}|^2 - 2)\beta_T x_2 \pm 2\sqrt{\pi}\int_{\zeta_1 \gtrless 0} \zeta_1 \phi E \, \mathrm{d}\boldsymbol{\zeta}, \qquad \text{for } \zeta_1 \lessgtr 0, \ x_1 = \pm\frac{1}{2}, \tag{2.2}$$

where

$$K(\phi) = \int \kappa(\boldsymbol{\zeta}_*, \boldsymbol{\zeta})\phi(\boldsymbol{\zeta}_*)E(|\boldsymbol{\zeta}_*|)\,\mathrm{d}\boldsymbol{\zeta}_*, \tag{2.3}$$

$$\kappa(\boldsymbol{\zeta}_*, \boldsymbol{\zeta}) = \frac{\sqrt{\pi}}{\sqrt{2}}\frac{1}{|\boldsymbol{\zeta} - \boldsymbol{\zeta}_*|}\exp\left(\frac{|\boldsymbol{\zeta}_* \times \boldsymbol{\zeta}|^2}{|\boldsymbol{\zeta}_* - \boldsymbol{\zeta}|^2}\right) - \frac{\sqrt{\pi}}{2\sqrt{2}}|\boldsymbol{\zeta} - \boldsymbol{\zeta}_*|, \tag{2.4}$$

$$\nu(|\boldsymbol{\zeta}|) = \frac{1}{2\sqrt{2}}\left[\exp(-|\boldsymbol{\zeta}|^2) + \left(2|\boldsymbol{\zeta}| + \frac{1}{|\boldsymbol{\zeta}|}\right)\int_0^{|\boldsymbol{\zeta}|}\exp(-s^2)\,\mathrm{d}s\right], \tag{2.5}$$

$$k = \frac{\sqrt{\pi}}{2}\frac{\ell_0}{D}, \quad \ell_0 = \frac{1}{\sqrt{2}\pi\sigma^2(\rho_0/m)}, \tag{2.6}$$

and ℓ_0 is the mean free path of a gas molecule at the reference equilibrium state. Note that we shall use k in place of the Knudsen number Kn ($=\ell_0/D$) to indicate the degree of gas rarefaction (see (2.6)). The above ϕ should be consistent with the imposed pressure field $p_0(1+\beta_P X_2/D)$, which is reduced to the following condition:

$$\frac{2}{3}\int |\boldsymbol{\zeta}|^2 \phi E \, \mathrm{d}\boldsymbol{\zeta} = \beta_P x_2. \tag{2.7}$$

Since the problem is linear, we can seek the solution ϕ, independent of x_3, in the form

$$\phi = \beta_P[x_2 + \phi_P(x_1, \boldsymbol{\zeta})] + \beta_T\left[\left(|\boldsymbol{\zeta}|^2 - \tfrac{5}{2}\right)x_2 + \phi_T(x_1, \boldsymbol{\zeta})\right], \tag{2.8}$$

where $\phi_J(x_1, \boldsymbol{\zeta})$ $(J = P,\ T)$ is a solution of the following boundary-value problem:

$$\zeta_1 \frac{\partial \phi_J}{\partial x_1} = -\frac{\nu}{k}\phi_J + \frac{1}{k}K(\phi_J) - I_J \quad (J = P, T), \tag{2.9a}$$

$$\phi_J = 0, \quad \text{for } \zeta_1 \lessgtr 0,\ x_1 = \pm\tfrac{1}{2}, \tag{2.9b}$$

$$I_P = \zeta_2, \quad I_T = \zeta_2\left(|\boldsymbol{\zeta}|^2 - \tfrac{5}{2}\right). \tag{2.9c}$$

Throughout this paper, the subscript J represents the problem indicator P or T: the former indicates the Poiseuille flow and the latter the thermal transpiration. Here ϕ_J is considered to be odd in ζ_2, even in ζ_3 and symmetric in the following sense:

$$\phi_J(x_1, \zeta_1, \zeta_2, \zeta_3) = \phi_J(-x_1, -\zeta_1, \zeta_2, \zeta_3). \tag{2.10}$$

Macroscopic quantities can be obtained once ϕ is known. Because of (2.8), the density, temperature, pressure and stress tensor of the gas are simply expressed as $\rho_0[1 + (\beta_P - \beta_T)x_2]$, $T_0(1 + \beta_T x_2)$, $p_0(1 + \beta_P x_2)$ and

$$p_0(1 + \beta_P x_2)\boldsymbol{I} - p_0\beta_P x_1 \begin{bmatrix} 0 & 1 & 0 \\ 1 & 0 & 0 \\ 0 & 0 & 0 \end{bmatrix} \qquad (\boldsymbol{I}\text{: the identity matrix}), \tag{2.11}$$

while the flow velocity $(2RT_0)^{1/2}\boldsymbol{u}$ and the heat flow vector $(1/2)\rho_0(2RT_0)^{3/2}\boldsymbol{Q}$ have their x_2-components only, which are expressed as a moment of ϕ as follows:

$$u_2 = \int \zeta_2 \phi E \, \mathrm{d}\boldsymbol{\zeta}, \quad Q_2 = \int \zeta_2 \left(|\boldsymbol{\zeta}|^2 - \frac{5}{2}\right) \phi E \, \mathrm{d}\boldsymbol{\zeta}. \tag{2.12}$$

For the sake of later convenience, we introduce the notation convention that

$$u[f] = \int \zeta_2 f E \, \mathrm{d}\boldsymbol{\zeta}, \quad Q[f] = \int \zeta_2 \left(|\boldsymbol{\zeta}|^2 - \frac{5}{2}\right) f E \, \mathrm{d}\boldsymbol{\zeta}, \quad M[f] = \int_{-1/2}^{1/2} u[f] \, \mathrm{d}x_1. \tag{2.13}$$

Then, u_2 and Q_2 may be rewritten by $u_2 = u[\phi] = \beta_P u[\phi_P] + \beta_T u[\phi_T]$ and $Q_2 = Q[\phi] = \beta_P Q[\phi_P] + \beta_T Q[\phi_T]$. The net mass flow through the channel per unit length in X_3 is expressed by $\rho_0 D(2RT_0)^{1/2} M[\phi]$, where $M[\phi] = \beta_P M[\phi_P] + \beta_T M[\phi_T]$.

3. Preliminary arguments

The problem (2.9) can be solved formally as

$$\phi_J = \phi_J^{(0)} + \phi_J^R, \tag{3.1a}$$

$$\phi_J^{(0)} = -\frac{k}{\nu}\left[1 - \exp\left(-\frac{\nu}{k}\frac{|x_1 \pm (1/2)|}{|\zeta_1|}\right)\right] I_J, \quad \zeta_1 \gtrless 0, \tag{3.1b}$$

$$\phi_J^R = \frac{1}{k\zeta_1}\int_{\mp 1/2}^{x_1} \exp\left(-\frac{\nu}{k}\frac{|s - x_1|}{|\zeta_1|}\right) K(\phi_J)\, \mathrm{d}s, \quad \zeta_1 \gtrless 0. \tag{3.1c}$$

In accordance with (3.1*a*), u, M and Q may be written as

$$u[\phi_J] = u\left[\phi_J^{(0)}\right] + u\left[\phi_J^R\right], \quad M[\phi_J] = M\left[\phi_J^{(0)}\right] + M\left[\phi_J^R\right], \quad Q[\phi_J] = Q\left[\phi_J^{(0)}\right] + Q\left[\phi_J^R\right]. \tag{3.2}$$

We primarily discuss the former two quantities; Q will be considered in § 6.2.

Chen *et al.* (2007) studied the thermal transpiration problem ϕ_T by the use of the formal solution (3.1) and proved mathematically the following for $k \gg 1$:

(i) There is a unique solution $\phi_T \in L^\infty$, where L^∞ is defined with the norm $\|f\|_\infty = \sup_\zeta |f|E^{1/2}$ for each x_1.

(ii) There is a constant $C > 0$ independent of k such that

$$|\phi_T E^{1/2}| \leqslant C\left(|\zeta_1| + \frac{1}{k}\right)^{-1}, \qquad |K(\phi_T)E^{1/2}| \leqslant C(1 + \ln k). \tag{3.3}$$

(iii) There are constants $C_2 \geqslant C_1 > 0$ and $C_3 > 0$ independent of k such that

$$C_1 \ln k \leqslant u\left[\phi_T^{(0)}\right] \leqslant C_2 \ln k, \qquad \left|u\left[\phi_T^R\right]\right| < C_3(1 + \ln k)^2/k. \tag{3.4}$$

The last estimate (3.4) implies that in the highly rarefied regime the flow $u[\phi_T^{(0)}]$ induced by the known inhomogeneous term corresponding to the temperature gradient is predominant, and the contribution of the remainder $u[\phi_T^R]$ is much smaller than $u[\phi_T^{(0)}]$, i.e. $O(k^{-1} \ln k)$ relative to $u[\phi_T^{(0)}]$. Since (3.4) is a uniform estimate in x_1, $M[\phi_T^R]$ and $M[\phi_T^{(0)}]$ follow the same estimate as (3.4).

By the analysis parallel to that of Chen *et al.* (2007), we can show for the Poiseuille flow problem that statements (i) and (ii) with ϕ_T being replaced by ϕ_P hold as they are and that (iii) is replaced by the following:

(iii)′ There are constants $C_2 \geqslant C_1 > 0$ and $C_3 > 0$ independent of k such that

$$-C_1 \ln k \geqslant u\left[\phi_P^{(0)}\right] \geqslant -C_2 \ln k, \qquad \left|u\left[\phi_P^R\right]\right| < C_3(1 + \ln k)^2/k \tag{3.5}$$

(see Appendix A). Again, because of the uniform estimate in x_1, $M[\phi_P^R]$ and $M[\phi_P^{(0)}]$ follow the same estimate as (3.5).

Remark. One may think that dropping the first two terms on the right-hand side of (2.9*a*) would give a reasonable approximation in the highly rarefied regime. It, however, leads to the divergence of flow velocity, which has been known for a long time. Physically, the divergence is caused by completely neglecting the scattering of molecules with a velocity parallel to the walls ($\zeta_1 = 0$). In the dominant part $\phi_J^{(0)}$ of the solution, the effect of such a scattering is partially included (only the term $K(\phi_J)/k$ is dropped from (2.9*a*)), which prevents the divergence for every fixed k and captures the asymptotic behaviour as $k \to \infty$. See, e.g., Cercignani (1988) and Sone (2007) for related discussions.

Figure 1 shows $M[\phi_J^{(0)}]$, the expression of which is eventually reduced to (4.6) that appears later. The direct numerical solution of $M[\phi_J]$ by Ohwada *et al.* (1989) is also shown for comparison. The relative error of $M[\phi_T^{(0)}]$ to $M[\phi_T]$ is less than 17 %, 13 % and 11 % for $k = 10$, 15 and 20, while that of $M[\phi_P^{(0)}]$ to $M[\phi_P]$ is less than 19 %, 15 % and 12 % for $k = 10$, 15 and 20. Thus, it is strongly suggested that the use of $\phi_J^{(0)}$ as the initial guess is effective for an iterative solution method in the highly rarefied regime.

4. Structure of the over-concentration and solution method

4.1. *Iterative approximation: method and error estimate*

Motivated by the result shown in figure 1, we consider a sequence of functions $\phi_J^{(0)}$, $\phi_J^{(1)}$, $\phi_J^{(2)}$, ... generated by the following procedure:

$$\phi_J^{(n)} = \phi_J^{(0)} + \int_{\mp 1/2}^{x_1} \frac{1}{k\zeta_1} \exp\left(-\frac{\nu}{k}\frac{|s - x_1|}{|\zeta_1|}\right) K\left(\phi_J^{(n-1)}\right) \mathrm{d}s, \quad \zeta_1 \gtrless 0, \quad (n = 1, 2, \ldots). \tag{4.1}$$

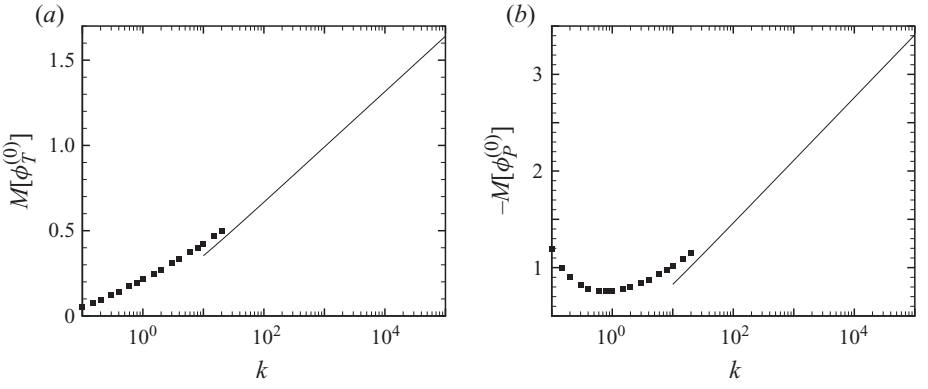

FIGURE 1. $M[\phi_J^{(0)}]$ for large Knudsen numbers. (*a*) $M[\phi_T^{(0)}]$ versus k and (*b*) $M[\phi_P^{(0)}]$ versus k. In each panel, $M[\phi_J^{(0)}]$ is shown by a solid line. Numerical results of $M[\phi_J]$ by Ohwada *et al.* (1989) for intermediate Knudsen numbers are also shown for comparison by the closed symbols.

By using both the norm and pointwise estimates following Chen *et al.* (2007), we can prove the following for $k \gg 1$ (see Appendix A):

(*a*) $\{\phi_J^{(n)}\}$ is a Cauchy sequence in L^∞ and thus has a limit in L^∞. Further, this limiting function is a solution of (3.1): $\phi_J = \lim_{n\to\infty} \phi_J^{(n)}$.

(*b*) By introducing $\psi_J^{(0)} = \phi_J^{(0)}$ and $\psi_J^{(n)} = \phi_J^{(n)} - \phi_J^{(n-1)}$ $(n = 1, 2, \ldots)$, $\phi_J^{(n)}$ is rewritten as $\phi_J^{(n)} = \sum_{i=0}^{n} \psi_J^{(i)}$. In order to have the sequence $\{\phi_J^{(n)}\}$, we may use the following generating procedure for $\{\psi_J^{(n)}\}$ in place of (4.1):

$$\psi_J^{(n)} = \int_{\mp 1/2}^{x_1} \frac{1}{k\zeta_1} \exp\left(-\frac{\nu}{k}\frac{|s - x_1|}{|\zeta_1|}\right) K\left(\psi_J^{(n-1)}\right) \mathrm{d}s, \quad \zeta_1 \gtrless 0. \tag{4.2}$$

Then there are positive constants C_0 and C_1 independent of k such that

$$\left|\psi_J^{(i)} E^{1/2}\right| \leqslant C_0(|\zeta_1| + k^{-1})^{-1}[C_1 k^{-1}(\ln k + 1)]^i, \tag{4.3a}$$

$$\left\| \psi_J^{(i)} \right\|_\infty \leqslant C_0 k[C_1 k^{-1}(\ln k + 1)]^i, \tag{4.3b}$$

$$\left|K\left(\psi_J^{(i)}\right) E^{1/2}\right| \leqslant C_0(\ln k + 1)\,[C_1 k^{-1}(\ln k + 1)]^i, \tag{4.3c}$$

where $i = 0, 1, 2, \ldots$. Thus the error of $\phi_J^{(i)} E^{1/2}$ is $O(k^{-i}(1 + \ln k)^{i+1})$.

(*c*) There are positive constants C_0 and C_1 independent of k such that

$$\left|u\left[\psi_J^{(i)}\right]\right|, \left|M\left[\psi_J^{(i)}\right]\right| \leqslant C_0[C_1 k^{-1}(\ln k + 1)]^i(\ln k + 1). \tag{4.4}$$

Remark. Equation (4.1) or (4.2) is a rather common iterative approximation procedure. Here the point is that we can prove (*a*)–(*c*) in the present problems, which have not been known so far. Incidentally, the above convergence rates (4.3*a*) and (4.4) of the sequences are faster than those suggested in remark 4.4 of Chen *et al.* (2007). This is because we make use of (4.3*c*) at each stage of iteration in the estimate (see Appendix A).

4.2. *Structure of over-concentration*

Estimate (4.3*a*) clearly shows the structure of the over-concentration of molecules on $\zeta_1 \sim 0$. Further, $\phi_J^{(0)} E^{1/2}$ (or $\psi_J^{(0)} E^{1/2}$) has a peak $O(k)$ around $\zeta_1 = 0$, remains $O(k)$

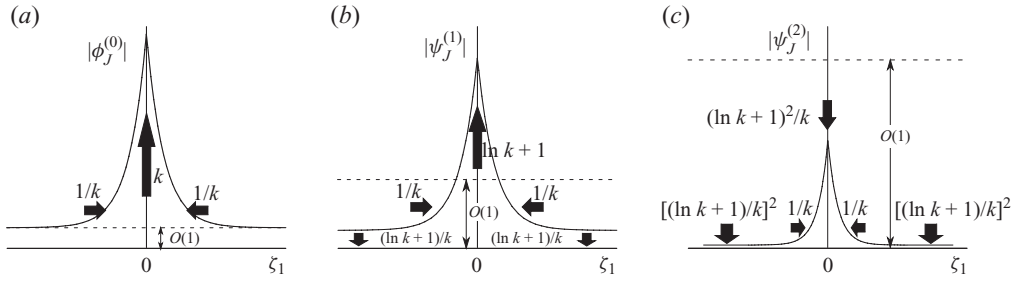

FIGURE 2. Change of (*a*) $\phi_J^{(0)}$, (*b*) $\psi_J^{(1)}$ and (*c*) $\psi_J^{(2)}$ for small $|\zeta_1|$ as k is increased ($k \gg 1$). In each panel, the rate and the direction of change when k is increased are shown.

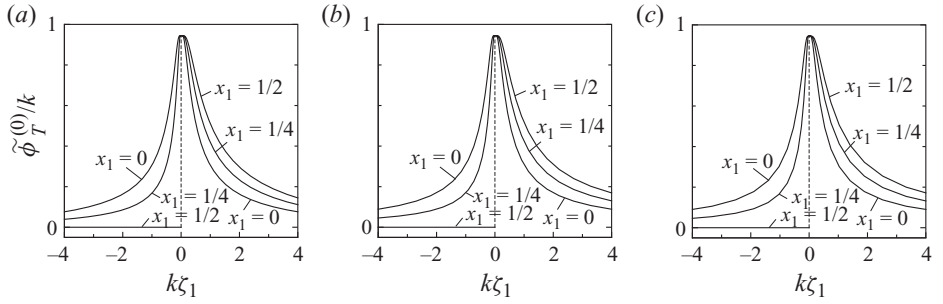

FIGURE 3. $\widetilde{\phi}_T^{(0)}/k$ versus $k\zeta_1$ at $\zeta_\rho = 0.611$ on three spatial points ($x_1 = 0$, 1/4 and 1/2), where $\zeta_\rho = (|\boldsymbol{\zeta}|^2 - \zeta_1^2)^{1/2}$. (*a*) $k = 10$, (*b*) $k = 10^2$ and (*c*) $k = 10^3$. Here, $\widetilde{\phi}_T^{(0)} \equiv \phi_T^{(0)} E^{1/2}/\zeta_2$ is a function of x_1, ζ_1 and ζ_ρ.

for $|\zeta_1| = O(k^{-1})$ and decreases down to $O(1)$ for $|\zeta_1| \sim 1$. As a result, its L^∞ norm, which picks up the peak value, is $O(k)$, while its averages such as $u[\phi_J^{(0)}]$ and $M[\phi_J^{(0)}]$ are smaller quantities $O(\ln k + 1)$. At each stage of iteration, $\psi_J^{(n)} E^{1/2}$ is scaled down by the factor $O(k^{-1}(\ln k + 1))$ with the peak position essentially unchanged.

In summary, the over-concentration in the highly rarefied regime occurs in the range of $|\zeta_1| = O(k^{-1})$. This phenomenon should be captured correctly by taking into account the first correction $\psi_J^{(1)}$ to the initial guess $\phi_J^{(0)}$ in the present iterative procedure, because $\psi_J^{(2)} E^{1/2}$ and higher-order corrections decrease with the rate $O(k^{-1}(\ln k + 1)^2)$ as k increased, as is clear from the above estimates. The feature is schematically shown in figure 2. Strictly speaking, estimate (4.3*a*) is not necessarily optimal, so that the actual peak and the range of over-concentration may be smaller and thinner than estimated. However, figure 3 and the data to be shown in § 5, which we obtained numerically, demonstrate that the estimate is actually optimal.

4.3. *Overview of computational method*

Most plainly, a straightforward iterative finite-difference scheme would be used for numerical computation, especially for intermediate Knudsen numbers. The scheme is obtained by discretizing in both x_1 and $\boldsymbol{\zeta}$ the following equation arising from (2.9):

$$\zeta_1 \frac{\partial \phi_J^{(n)}}{\partial x_1} = -\frac{\nu}{k}\phi_J^{(n)} + \frac{1}{k} K\left(\phi_J^{(n-1)}\right) - I_J, \tag{4.5a}$$

$$\phi_J^{(n)} = 0, \qquad \text{for } \zeta_1 \lessgtr 0, \ x_1 = \pm\tfrac{1}{2}. \tag{4.5b}$$

Equation (4.1), which was the basis of the discussion of § 4.2, is also obtained by analytical integration of (4.5) with respect to x_1. Thus, the sequence of functions $\phi_J^{(0)}, \phi_J^{(1)}, \ldots$ generated by (4.1) is identical to that generated by (4.5) with $\phi_J^{(-1)} = 0$. Thus, the finite-difference scheme that is based on (4.5) should converge also with the rate $O(k^{-1}(\ln k + 1))$ in the highly rarefied regime, which actually gives a numerical solution in that regime only by several (or even a few) iterations. Nevertheless, the straightforward finite-difference approach will be faced with a difficulty. The difficulty lies in the discretization. As described before, $M[\phi_J]$ is a quantity $O(\ln k)$ (see (3.4) and (3.5)). The contribution from the region in ζ_1 where ϕ_J decreases down from $O(k)$ to $O(1)$ is $O(\ln k)$, while the contribution from the remaining region is $O(1)$ (see (3.3)). Thus, a well-balanced arrangement of grid points both to the thin over-concentration part and to the remaining part is required, which becomes difficult to realize for large k, especially when the knowledge in § 4.2 is lacking. (Note that, in practice, $\ln k$ is not so different from 1 when k is large. Compare 1, $\ln k$ and k when $k = 10^3$.)

Because of the above observation, we carry out the numerical computations in the following way. Here the main concern is the net mass flow $M[\phi_J]$. We first calculate the zeroth and first approximations, which are responsible for the over-concentration, analytically as much as possible. In this step, thanks to the simple form of $\phi_J^{(0)}$ (see (3.1*b*)), $M[\phi_J^{(0)}]$ is eventually reduced to

$$M\left[\phi_J^{(0)}\right] = \frac{1}{\sqrt{\pi}} \int_0^\infty \left[\left(1 - \frac{a^2}{12k^2}\right) \mathrm{Ei}\left(-\frac{a}{k}\right) + \frac{1}{12}\left(1 - \frac{a}{k}\right) \mathrm{e}^{-\frac{a}{k}} - \frac{1}{2}\frac{k}{a}\left\{1 + \left(\frac{5}{3} - \frac{k}{a}\right)\left(1 - \mathrm{e}^{-\frac{a}{k}}\right)\right\}\right] t^3 \tilde{I}_J \mathrm{e}^{-t^2} \mathrm{d}t, \quad (4.6)$$

where Ei is the exponential integral defined by $\mathrm{Ei}(-x) = -\int_x^\infty t^{-1}\exp(-t)\mathrm{d}t$ $(x > 0)$ and

$$a = \frac{\nu(t)}{t}, \quad \tilde{I}_P = 1, \quad \tilde{I}_T = \left(t^2 - \frac{5}{2}\right). \quad (4.7)$$

The remaining integration with respect to t is easily performed numerically. The results shown in figure 1 are thus obtained. For $n \geqslant 1$, $\psi_J^{(n)}$ is expressed by (4.2). The corresponding net mass flow is expressed as

$$M\left[\psi_J^{(n)}\right] = 2\int_{-1/2}^{1/2} \int_{\zeta_1 > 0} \frac{\zeta_2}{\nu}\left(1 - \exp\left(-\frac{\nu}{k}\frac{(1/2) - s}{\zeta_1}\right)\right) K\left(\psi_J^{(n-1)}\right) E(|\boldsymbol{\zeta}|)\,\mathrm{d}\boldsymbol{\zeta}\,\mathrm{d}s, \quad (4.8)$$

because the integration with respect to x_1 from $-1/2$ to $1/2$ can be performed analytically after changing the order of integration. As to $\psi_J^{(1)}$ and $M[\psi_J^{(1)}]$, the integration with respect to s and a part of the others can be performed analytically, thanks to the simple form of $\phi_J^{(0)}$ (see (3.1*b*)). As a result, (4.2) and (4.8) are eventually reduced to three- and fivefold integrations of a given function respectively. These integrations are performed numerically by first applying the double exponential transformation (Takahasi & Mori 1974; Mori & Sugihara 2001; Mori 2005) and then using the trapezoid formula for transformed variables.

By the method in the previous paragraph, we can deal with the over-concentration and its contribution to the net mass flow accurately. In the extremely highly rarefied regime, the first (or even zeroth) approximation is accurate enough, thanks to the convergence rate $O(k^{-1}(\ln k + 1))$ in one iteration. Further iterations are required only in the regime close to the intermediate rarefied regime. The required number of iterations increases as k is decreased, because the convergence rate $O(k^{-1}(\ln k + 1))$

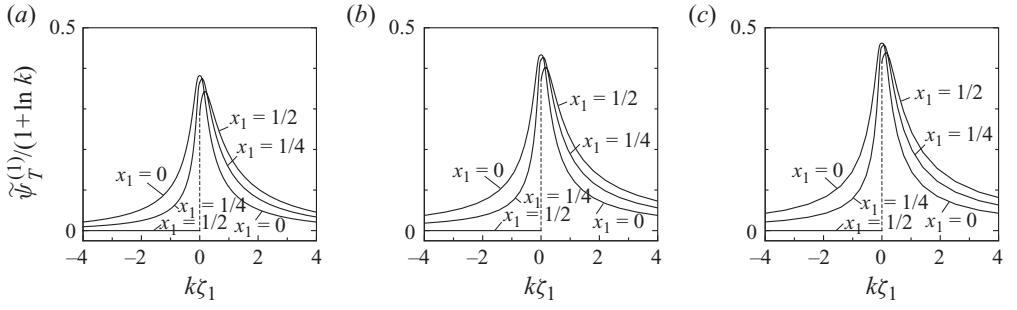

FIGURE 4. $\widetilde{\psi}_T^{(1)}/(1+\ln k)$ versus $k\zeta_1$ at $\zeta_\rho = 0.611$ $[\zeta_\rho = (|\boldsymbol{\zeta}|^2 - \zeta_1^2)^{1/2}]$ on three spatial points ($x_1 = 0$, 1/4 and 1/2), where $\widetilde{\psi}_T^{(1)} \equiv \psi_T^{(1)} E^{1/2}/\zeta_2$ is a function of x_1, ζ_1 and ζ_ρ. (*a*) $k = 10$, (*b*) $k = 10^2$ and (*c*) $k = 10^3$.

becomes worse. Fortunately, however, we do not expect a serious numerical difficulty in that regime, because the range of the over-concentration in ζ_1, which is $O(k^{-1})$, is no longer too thin. The main technical problem in solving $\psi_J^{(2)}$ and higher-order corrections is that only the discretized data of $\psi_J^{(n-1)}$ are available in (4.2) and (4.8) and that the integration with respect to s cannot be carried out analytically. The integration with respect to $\boldsymbol{\zeta}$ is performed by using the trapezoid formula after the double exponential transformation. As to the integration with respect to s, $K(\psi_J^{(n-1)})$ is approximated by the piecewise quadratic interpolation of the data on grid points. Then the integration of the approximated $K(\psi_J^{(n-1)})$ multiplied by $1 - \exp(-\nu((1/2) - s)/(k\zeta_1))$ in (4.8) or $\exp(-\nu|s - x_1|/(k|\zeta_1|))$ in (4.2) is carried out analytically. In the actual numerical computations, we seek $\psi_J^{(n)}(x_1, \boldsymbol{\zeta})$ in the form of $(\zeta_2/\zeta_\rho)\Psi_J^{(n)}(x_1, \zeta_1, \zeta_\rho)$ ($\zeta_\rho = \sqrt{|\boldsymbol{\zeta}|^2 - \zeta_1^2}$), following Ohwada *et al.* (1989). The same similarity applies to $K(\psi_J^{(n)})$. Thus, the computations have been carried out for functions of x_1, ζ_1 and ζ_ρ. In the computations, 11, 97 and 113 grid points have been arranged in the half-ranges of x_1 and ζ_1 (i.e. $0 \leqslant x_1 \leqslant 1/2$ and $\zeta_1 > 0$) and in the whole range of $\zeta_\rho (> 0)$. Grid points in $-1/2 \leqslant x_1 \leqslant 0$ and $\zeta_1 < 0$ have been arranged symmetrically with respect to $x_1 = 0$ and $\zeta_1 = 0$.

5. Numerical results and discussions

5.1. *Velocity distribution functions*

Figures 4 and 5 show an example of $\psi_T^{(1)}$ and $K(\phi_T^{(0)})$ obtained numerically. The behaviour of $K(\phi_T^{(0)})$ and $\psi_T^{(1)}$ in the figures actually follows estimate (4.3). That is, as is seen in figure 4, $\psi_T^{(1)}$ is $O(\ln k + 1)$ and is localized in the range of $|k\zeta_1| \lesssim 1$. On the other hand, as is seen in figure 5, $K(\phi_T^{(0)})$ is also $O(\ln k + 1)$, but there is no trace of the over-concentration observed in $\phi_T^{(0)}$; i.e. $K(\phi_T^{(0)})$ behaves moderately in ζ_1. These facts mean that the localization of $\phi_T^{(0)}$ disappears by the action of K but is reproduced by the action of integration (4.2). Note that $\psi_T^{(1)}$ and $\phi_T^{(0)}$ are similar to each other (see figures 3 and 4). Thus, roughly speaking, with the action of integration (4.2) after K as a unit process, the original distribution is reproduced with the scale reduced by the factor of $k^{-1}(\ln k + 1)$. Figure 6 shows the transition from $\phi_T^{(0)}$ to $\psi_T^{(4)}$ that is obtained numerically for $k = 10$. The figure shows the expected invariance of

	Present results							
	Thermal transpiration			Poiseuille flow			Literature[a]	
k	$M[\phi_T^{(0)}]$	$M[\phi_T^{(1)}]$	$M[\phi_T^{(n)}]$	$M[\phi_P^{(0)}]$	$M[\phi_P^{(1)}]$	$M[\phi_P^{(n)}]$	$M[\phi_T]$	$M[\phi_P]$
10	0.3530	0.4117	$0.4241^{(7)b}$	−0.8267	−0.9805	$-1.0159^{(7)}$	0.4241	−1.0159
15	0.4064	–	–	−0.9360	–	–	0.4668	−1.0907
20	0.4451	0.4924	$0.4982^{(5)}$	−1.0146	−1.1322	$-1.1477^{(5)}$	0.4982	−1.1477
10^2	0.6673	0.6893	$0.6900^{(3)}$	−1.4621	−1.5125	$-1.5143^{(3)}$	–	–
10^3	0.9910	0.9960	$0.9960^{(2)}$	−2.1102	−2.1210	$-2.1210^{(2)}$	–	–
10^4	1.3157	1.3166	$1.3166^{(1)}$	−2.7596	−2.7615	$-2.7615^{(1)}$	–	–
10^5	1.6404	1.6406	$1.6406^{(1)}$	−3.4091	−3.4094	$-3.4094^{(1)}$	–	–
10^6	1.9652	1.9652	$1.9652^{(1)}$	−4.0587	−4.0587	$-4.0587^{(1)}$	–	–

[a]Direct numerical solution by Ohwada *et al.* (1989). The data refined by Kosuge *et al.* (2005), which may differ at most by 2 at the last digit from those of Ohwada *et al.* (1989), are shown in the table.
[b]Converged data. The superscript number in parentheses indicates the order of approximation n.

TABLE 1. Net mass flows in the highly rarefied regime.

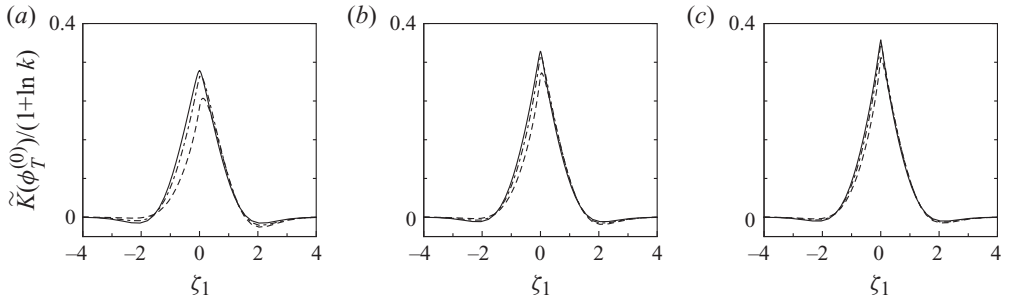

FIGURE 5. $\widetilde{K}(\phi_T^{(0)})/(1+\ln k)$ versus ζ_1 at $\zeta_\rho = 0.611$ $[\zeta_\rho = (|\boldsymbol{\zeta}|^2 - \zeta_1^2)^{1/2}]$ on three spatial points ($x_1 = 0$, 1/4 and 1/2), where $\widetilde{K}(\phi_T^{(0)}) \equiv K(\phi_T^{(0)})E^{1/2}/\zeta_2$ is a function of x_1, ζ_1 and ζ_ρ. (*a*) $k = 10$, (*b*) $k = 10^2$ and (*c*) $k = 10^3$. In each panel, the solid, dash-dotted and dashed lines indicate the profile at $x_1 = 0$, 0.25 and 0.5, respectively.

the form of $\psi_J^{(n)}$ in the iterative process. This implies that estimate (4.3*a*) is actually optimal, as mentioned at the end of § 4.2.

5.2. *Net mass flows*

The net mass flows that have been obtained numerically for several values of k are shown in table 1. In table 1, the zeroth-, first- and higher-order iterative approximation solutions ($M[\phi_J^{(0)}]$, $M[\phi_J^{(1)}]$ and $M[\phi_J^{(n)}]$) are presented, where the data in the columns of $M[\phi_J^{(n)}]$ have converged to five digits. We have also prepared a database that promptly gives the net mass flows for arbitrary values of $k \geqslant 10$ in the same way as Kosuge & Takata (2008). The details are given in Appendix B. The data taken from the database are shown by the solid lines in figure 7, together with the numerical results by Ohwada *et al.* (1989) and Kosuge *et al.* (2005) for intermediate Knudsen numbers (open symbols), the asymptotic solutions in Sone (2007) for small Knudsen numbers (dash-dotted lines) and the asymptotic formula (6.1) for large Knudsen numbers that appears later (dashed lines). As is clear from the table and the figure, the present results (solid lines) are smoothly connected to those of Ohwada *et al.*

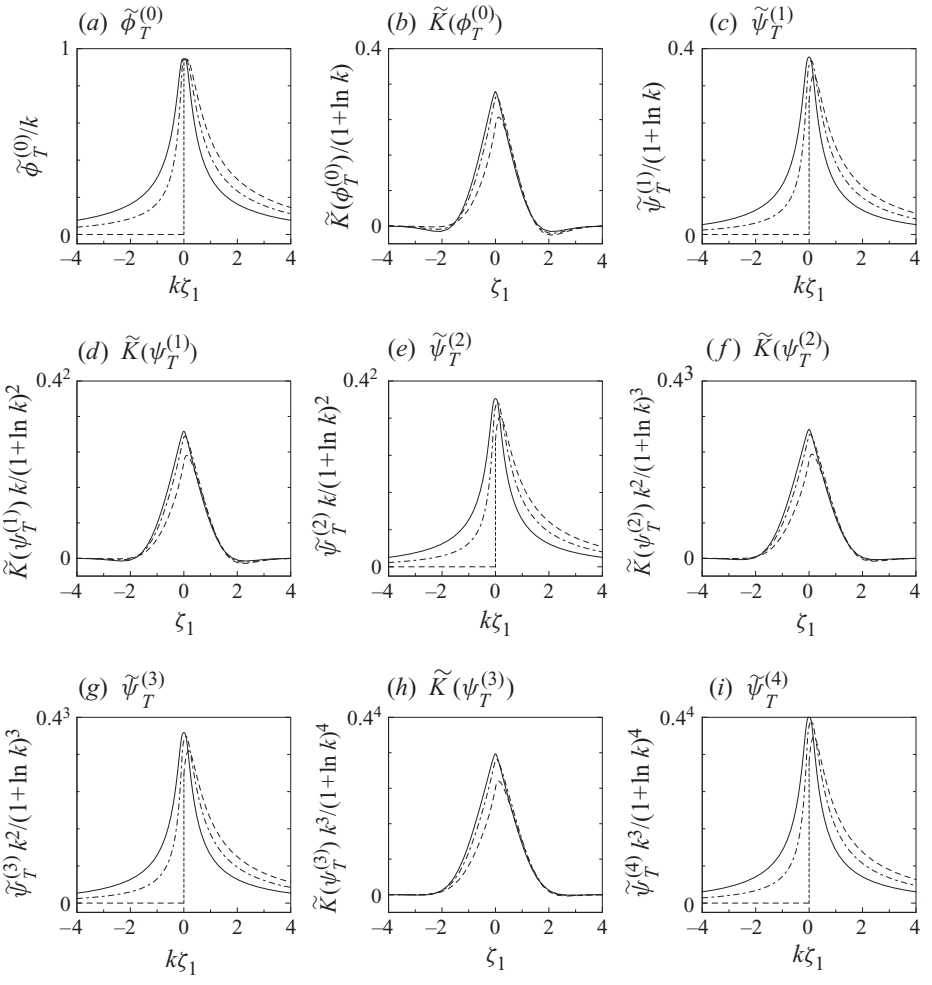

FIGURE 6. Transition from $\phi_T^{(0)}$ to $\psi_T^{(4)}$ ($\phi_T^{(0)} \to K(\phi_T^{(0)}) \to \psi_T^{(1)} \to K(\psi_T^{(1)}) \to \psi_T^{(2)} \to K(\psi_T^{(2)}) \to \psi_T^{(3)} \to K(\psi_T^{(3)}) \to \psi_T^{(4)}$) in the case of $k = 10$ at $\zeta_\rho = 0.611$ ($\zeta_\rho = (|\boldsymbol{\zeta}|^2 - \zeta_1^2)^{1/2}$). In each panel, rescaled $\widetilde{\phi}_T^{(0)} = \phi_T^{(0)} E^{1/2}/\zeta_2$, $\widetilde{\psi}_T^{(n)} = \psi_T^{(n)} E^{1/2}/\zeta_2$ ($n = 1, \ldots, 4$) or $\widetilde{K}(\cdot) = K(\cdot)E^{1/2}/\zeta_2$, which is a function of x_1, ζ_1 and ζ_ρ, is shown in place of $\phi_T^{(0)}$, $\psi_T^{(n)}$ or $K(\cdot)$. The solid, dash-dotted and dashed lines indicate the profile at $x_1 = 0$, 0.25 and 0.5, respectively. Note the difference of the scale of abscissa between two groups of panels, i.e. (*a*), (*c*), (*e*), (*g*) and (*i*) versus (*b*), (*d*), (*f*) and (*h*). The factor 0.4 in the ordinate corresponds to the constant C_1 in (4.3).

(1989) and Kosuge *et al.* (2005) for intermediate Knudsen numbers. (Kosuge *et al.* 2005, who studied the case of binary gas mixtures, obtained the data for a pure gas as a special case, though they are not shown in the paper. Those data are mentioned when the work of Kosuge *et al.* 2005 is cited in the present paper.)

6. Further discussions on asymptotic behaviour as $k \to \infty$

6.1. *Grad's hard potential and asymptotic formula for $M[\phi_J]$*

In obtaining (4.6), we have changed the order of integration, which is allowed because there is a positive constant ν_* such that $\nu \geqslant \nu_* > 0$. Expression (4.6) is valid for

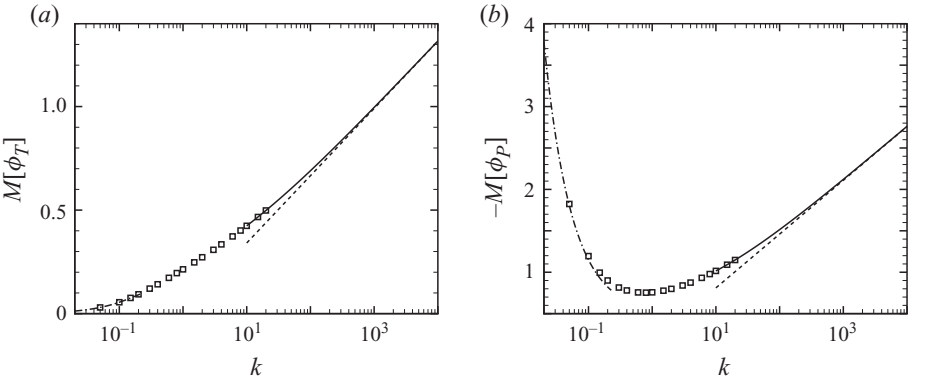

FIGURE 7. Net mass flows as a function of k. (*a*) $M[\phi_T]$ versus k and (*b*) $M[\phi_P]$ versus k. The solid lines indicate the data taken from the present database (see (B 1)), the dashed lines the asymptotic formula (6.1*a*), the dash-dotted lines the asymptotic theory for small k (Sone 2007) and the open symbols the numerical data by Ohwada *et al.* (1989) and Kosuge *et al.* (2005).

any molecular model if its $\nu(|\boldsymbol{\zeta}|)$ has a positive lower bound. Grad (1963) showed that such a positive lower bound exists for his hard-potential model (Grad's hard potential; see Appendix C), which contains the HS model as a special case. Further, by using the mathematical estimates of Grad (1963), we can show that estimates (*a*)–(*c*) in § 4.1 are valid also for Grad's hard potential. Thus, the discussion so far also applies to Grad's hard potential. Besides the HS model, various practical models such as the cutoff inverse-power-law (IPL) model with the exponent $s \geqslant 5$ ($s = 5$ is the cutoff Maxwell molecule), the variable hard-sphere (VHS) model (Bird 1994) with the viscosity index $1/2 \leqslant \omega \leqslant 1$ and the variable soft-sphere (VSS) model (Koura & Matsumoto 1991) with $1/2 \leqslant \omega \leqslant 1$ and the exponent of cosine of deflection angle $\alpha \geqslant 1$ belong to Grad's hard potential. (As to the notation ω and α we follow Bird 1994, while as to s we follow Grad 1963. The viscosity index of the IPL model with the exponent s is given by $\omega = (s + 3)/[2(s - 1)]$.)

One useful consequence of the above facts is that $M[\phi_J]$ can be expressed by the right-hand side of (4.6) for any molecular model belonging to Grad's hard potential within the error $O(k^{-1}(\ln k)^2)$. Examining the behaviour of the integrand in (4.6) as $k \to \infty$ leads to the following simple asymptotic formula for $M[\phi_J]$ for Grad's hard potential:

$$M[\phi_J] = C_{J0} \ln k + C_{J1} + C_J[\nu] + O(k^{-1}(\ln k)^2), \tag{6.1a}$$

where

$$C_{P0} = -\frac{1}{2\sqrt{\pi}}, \quad C_{P1} = -\frac{3}{4}\frac{1}{\sqrt{\pi}}(1 - \gamma), \quad C_{T0} = \frac{1}{4\sqrt{\pi}}, \quad C_{T1} = \frac{1}{8\sqrt{\pi}}(1 - 3\gamma), \tag{6.1b}$$

$$C_J[\nu] = \frac{1}{\sqrt{\pi}} \int_0^\infty t^3 \ln \nu(t) \tilde{I}_J \mathrm{e}^{-t^2} \, \mathrm{d}t, \tag{6.1c}$$

and γ is the Euler constant ($\gamma = 0.577216$). Note that C_{P0} and C_{T0} are independent of molecular models. Thus, as far as the leading order is concerned, $M[\phi_J]$ is independent of molecular models in the highly rarefied regime. This is not obvious from (3.1*b*).

Molecular model	Viscosity index ω^a	$\sqrt{\pi}C_P[\nu]$	$\sqrt{\pi}C_T[\nu]$
HS	1/2	0.0310229	0.120791
VHS (helium or neon)	0.66	0.0237010	0.0832157
VHS (argon)	0.81	0.0147201	0.0471379
VHS (xenon)	0.85	0.0119477	0.0373583
Pseudo-Maxwell	1	0	0

[a]Taken from table A1 in Bird (1994).

TABLE 2. Coefficients $C_P[\nu]$ and $C_T[\nu]$ in (6.1).

Further, $C_P[\nu]$ and $C_T[\nu]$ can be obtained easily. Some examples are shown in table 2, where ν is normalized in such a way that $\overline{\nu}$ defined by $\overline{\nu} := (4/\sqrt{\pi})\int_0^\infty t^2\nu(t)\mathrm{e}^{-t^2}\,\mathrm{d}t$ is unity. For instance, for the VHS and IPL models with the viscosity index ω, ν is commonly given by

$$\nu(t) = \frac{2^{\omega-2}}{\Gamma(-\omega+(5/2))}\frac{1}{t}\int_0^\infty r^{3-2\omega}(\exp(-|t-r|^2)-\exp(-|t+r|^2))\,\mathrm{d}r. \tag{6.2}$$

Thus, formula (6.1*a*) for the VHS model is identical to that for the IPL model with the same viscosity index. They can be different from each other at $O(k^{-1}(\ln k)^2)$ or higher order of k^{-1}, because of the difference of K in (2.9*a*). Incidentally, if ν is normalized in such a way that $\overline{\nu}\neq 1$, we rewrite (6.1*a*) as $M[\phi_J] = C_{J0}\ln(k/\overline{\nu}) + C_{J1} + C_J[\nu/\overline{\nu}] + O(k^{-1}(\ln k)^2)$ and identify the values of $\sqrt{\pi}C_J[\nu/\overline{\nu}]$ with those of $\sqrt{\pi}C_J[\nu]$ in table 2.

In the case of the HS model, the actual error of formula (6.1) (the first three terms) is less than 20 %, 3.6 %, 0.52 % and 0.073 % for $k = 10$, 10^2, 10^3 and 10^4, respectively. For $k \geqslant 10^4$, formula (6.1) gives the same values as those of $M[\phi_J^{(0)}]$ at least to five digits.

The asymptotic formula corresponding to (6.1) can be obtained along the same lines for Poiseuille and thermal transpiration flows in a circular tube. Let us denote by D a radius of the pipe cross-section and by $\rho_0(\pi D^2)(2RT_0)^{1/2}M[\phi]$ the net mass flow through the pipe cross-section, where ϕ is written as $\phi = \beta_P[x_2+\phi_P(x_1,x_3,\boldsymbol{\zeta})] + \beta_T[(|\boldsymbol{\zeta}|^2-(5/2))x_2+\phi_T(x_1,x_3,\boldsymbol{\zeta})]$. Then, we can show that $M[\phi_J]$ is given by

$$M[\phi_P] = -\frac{4}{3}\frac{1}{\sqrt{\pi}} + O(k^{-1}\ln k), \quad M[\phi_T] = \frac{2}{3\sqrt{\pi}} + O(k^{-1}\ln k), \tag{6.3}$$

for $k \gg 1$, irrespective of the molecular model as long as it belongs to Grad's hard potential. It should be noted that (6.3) agrees with the classical results for the BGK model, including the order of the error terms (Cercignani & Sernagiotto 1966; Niimi 1968; see also Kennard 1938).

6.2. *Similarity between $u[\phi_T]$ and $Q[\phi_P]$*

It is known that the dimensionless net mass flow of the thermal transpiration is identical to the dimensionless net heat flow of the Poiseuille flow for arbitrary Knudsen numbers (Loyalka 1971; see also Takata 2009):

$$\int_{-1/2}^{1/2} u[\phi_T]\,\mathrm{d}x_1 = \int_{-1/2}^{1/2} Q[\phi_P]\,\mathrm{d}x_1. \tag{6.4}$$

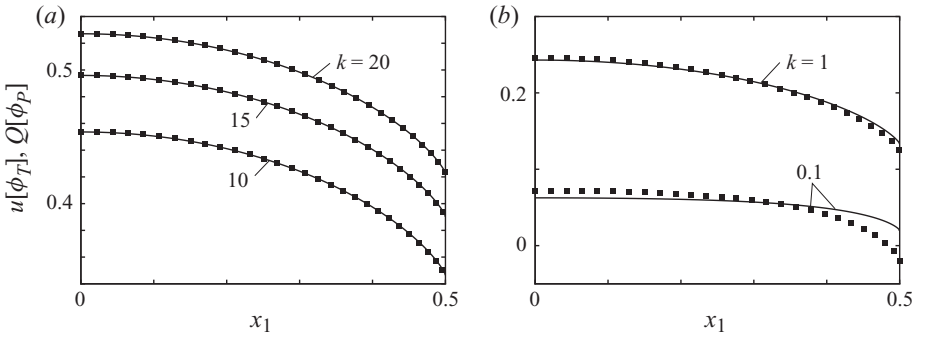

FIGURE 8. Profiles of $u[\phi_T]$ and $Q[\phi_P]$ in the half-range of the channel ($0 \leqslant x_1 \leqslant 1/2$). (*a*) Large k and (*b*) small and intermediate k. The solid lines indicate $u[\phi_T]$, while the closed symbols indicate $Q[\phi_P]$. The data shown were obtained by Kosuge *et al.* (2005).

It is, however, seen from (3.1*b*) that $u[\phi_T^{(0)}]$ and $Q[\phi_P^{(0)}]$ are identical even at the level of spatial profile:

$$u\left[\phi_T^{(0)}\right] = Q\left[\phi_P^{(0)}\right]. \tag{6.5}$$

That is, the profile of dimensionless flow velocity of thermal transpiration agrees with that of dimensionless heat flow of Poiseuille flow within the error $O(k^{-1}(\ln k)^2)$ for large k:

$$u[\phi_T] = Q[\phi_P] + O(k^{-1}(\ln k)^2) \qquad (k \gg 1). \tag{6.6}$$

Figure 8(*a*) shows the profiles of $u[\phi_T]$ and $Q[\phi_P]$ for $k = 10$, 15 and 20 obtained by Kosuge *et al.* (2005). In the figure, $u[\phi_T]$ is indicated by the solid lines, while $Q[\phi_P]$ is indicated by the closed symbols. They agree well with each other, which is explained by relation (6.6). As shown in figure 8(*b*), the profiles do not agree for small and intermediate Knudsen numbers.

7. Conclusion

In the present paper, we have investigated the Poiseuille and thermal transpiration flows of a highly rarefied gas, with a special interest in the over-concentration of molecules on velocities parallel to the walls. Making use of the mathematical estimate given in Chen *et al.* (2007) and Grad (1963), we have constructed an iterative approximation scheme with an explicit convergence estimate for the highly rarefied regime and have clarified the structure of the over-concentration in the velocity distribution function. We have also constructed a database for both problems that promptly gives the accurate data of the net mass flow for an arbitrary value of $k \geqslant 10$ for an HS molecular gas. In addition, we have presented an explicit simple asymptotic formula for the net mass flows for large Knudsen numbers, which is valid up to $O(1)$ and is applicable to any molecular model belonging to Grad's hard potential. Finally, we have pointed out that the profiles of the heat flow of Poiseuille flow and of the flow velocity of thermal transpiration agree with each other in the highly rarefied regime and have clarified the reason.

Appendix A. Sketch of proofs of the statements in §§ 3 and 4.1

The difference between the Poiseuille flow and thermal transpiration problems lies only in the form of I_J. This difference requires a few minor changes in the course of

the proof in Chen *et al.* (2007) to reach statements (i), (ii) and (iii)′ of § 3. Thus, we shall provide below only the sketch of proof of the statements in § 4.1.

Part (*b*). By using lemma 4.2 of Chen *et al.* (2007), we first easily obtain that there is a positive constant C_0 such that

$$|\psi_J^{(0)} E^{1/2}| \leqslant C_0 \left(\frac{1}{k} + |\zeta_1|\right)^{-1}, \quad \left\| \psi_J^{(0)} \right\|_\infty \leqslant C_0 k, \tag{A 1}$$

where $\|\cdot\|_\infty = \sup_\zeta |\cdot E^{1/2}|$. Then, by following the proof of lemma 4.3 of Chen *et al.* (2007), we have from the above estimate that there is a positive constant C such that

$$|K(\psi_J^{(0)}) E^{1/2}| \leqslant C C_0 (\ln k + 1). \tag{A 2}$$

Using this estimate in (4.2), we obtain

$$|\psi_J^{(1)} E^{1/2}| \leqslant C_0^2 C k^{-1} (\ln k + 1) \left(\frac{1}{k} + |\zeta_1|\right)^{-1}, \quad \left\| \psi_J^{(1)} \right\|_\infty \leqslant C_0^2 C (\ln k + 1). \tag{A 3}$$

Note that $\psi_J^{(1)}$ follows the same estimate as $\psi_J^{(0)}$ as a function of $\boldsymbol{\zeta}$ and x_1. Thus, by repeating the above process, we have

$$\left| K\left(\psi_J^{(1)}\right) E^{1/2} \right| \leqslant (C C_0)^2 k^{-1} (\ln k + 1)^2 \tag{A 4}$$

and further conclude (4.3) in § 4.1. (The $\max(C_0, C C_0)$ and $C C_0$ here are the C_0 and C_1 in (4.3).) Since the above constants C and C_0 are independent of k, $\|\psi_J^{(n)}\|_\infty \to 0$ as $n \to \infty$.

Part (*a*). By the use of estimate (4.3*a*), we see that $\|\phi_J^{(n)}\|_\infty \leqslant C_0 k / [1 - C C_0 k^{-1} (\ln k + 1)] < \infty$ and that $\forall n > m$,

$$\left| \left(\phi_J^{(n)} - \phi_J^{(m)}\right) E^{1/2} \right| \leqslant C_0 \left(\frac{1}{k} + |\zeta_1|\right)^{-1} \frac{[C C_0 k^{-1} (\ln k + 1)]^{m+1}}{1 - C C_0 k^{-1} (\ln k + 1)}. \tag{A 5}$$

For sufficiently large k, the right-hand side tends to zero as $m \to \infty$, so that $\|\phi_J^{(n)} - \phi_J^{(m)}\|_\infty \to 0$. Thus $\{\phi_J^{(n)}\}$ is a Cauchy sequence in L^∞. Now denote $\lim_{n\to\infty} \phi_J^{(n)}$ by Φ_J and define a function R_J by

$$R_J \equiv \Phi_J - \phi_J^{(0)} - \int_{\mp 1/2}^{x_1} \frac{1}{k\zeta_1} \exp\left(-\frac{\nu}{k} \frac{|s - x_1|}{|\zeta_1|}\right) K(\Phi_J)\, \mathrm{d}s, \quad \zeta_1 \gtrless 0. \tag{A 6}$$

Since this equation can be rewritten as

$$R_J = \Phi_J - \phi_J^{(n)} - \int_{\mp 1/2}^{x_1} \frac{1}{k\zeta_1} \exp\left(-\frac{\nu}{k} \frac{|s - x_1|}{|\zeta_1|}\right) K\left(\Phi_J - \phi_J^{(n-1)}\right) \mathrm{d}s, \quad \zeta_1 \gtrless 0, \tag{A 7}$$

we obtain $\|R_J\|_\infty \leqslant \|\Phi_J - \phi_J^{(n)}\|_\infty + C_0 \|K(\Phi_J - \phi_J^{(n-1)})\|_\infty \to 0$ as $n \to \infty$, where lemma 4.1 of Chen *et al.* (2007) has been used. Thus Φ_J is a solution of (3.1) in L^∞.

Part (*c*). First, $u[\psi_J^{(n)}]$ is expressed as

$$\begin{aligned} u[\psi_J^{(n)}] = &\int_{-\infty}^{\infty} \int_{-\infty}^{\infty} \int_{0}^{\infty} \int_{-1/2}^{x_1} \frac{\zeta_2}{\zeta_1} \exp\left(-\frac{\nu}{k|\zeta_1|} |s - x_1|\right) \frac{1}{k} K\left(\psi_J^{(n-1)}\right) E \, \mathrm{d}s \, \mathrm{d}\zeta_1 \, \mathrm{d}\zeta_2 \, \mathrm{d}\zeta_3 \\ &+ \int_{-\infty}^{\infty} \int_{-\infty}^{\infty} \int_{-\infty}^{0} \int_{1/2}^{x_1} \frac{\zeta_2}{\zeta_1} \exp\left(-\frac{\nu}{k|\zeta_1|} |s - x_1|\right) \frac{1}{k} K\left(\psi_J^{(n-1)}\right) E \, \mathrm{d}s \, \mathrm{d}\zeta_1 \, \mathrm{d}\zeta_2 \, \mathrm{d}\zeta_3. \end{aligned} \tag{A 8}$$

j	$a_P^{(j)}$	$a_T^{(j)}$	j	$a_P^{(j)}$	$a_T^{(j)}$
0	−1.84790018(+0)[a]	8.54825701(−1)	9	1.49228707(−7)	−1.25559087(−7)
1	−8.83316631(−1)	4.49679688(−1)	10	2.60089118(−7)	−8.99270022(−8)
2	−3.92650101(−2)	1.52324109(−2)	11	−1.14839592(−7)	3.11987783(−8)
3	1.05217018(−2)	−3.54414570(−3)	12	−2.17698962(−8)	8.08859477(−9)
4	−1.57787850(−3)	3.01542071(−4)	13	9.70450516(−8)	−3.18197288(−8)
5	2.70953882(−5)	8.62335466(−5)	14	−2.15201321(−7)	6.99137082(−8)
6	3.90220820(−5)	−3.32236013(−5)	15	2.68421948(−7)	−1.00798691(−7)
7	−5.19294709(−6)	3.56117808(−6)	16	−1.68935567(−7)	5.64147556(−8)
8	−1.00587844(−6)	5.59709749(−7)			

[a]Read as $-1.84790018 \times 10^{+0}$.

TABLE 3. Coefficients $a_P^{(j)}$ and $a_T^{(j)}$ in (B 1) for $10 \leqslant k < 10^4$.

j	$a_P^{(j)}$	$a_T^{(j)}$	j	$a_P^{(j)}$	$a_T^{(j)}$
0	−3.73438354(+0)[a]	1.80303014(+0)	5	1.25230608(−5)	−5.76967764(−6)
1	−9.73557111(−1)	4.86790137(−1)	6	−2.45021285(−6)	1.09473993(−6)
2	−4.16662892(−4)	2.00691591(−4)	7	3.79936917(−7)	−1.61013000(−7)
3	1.66673351(−4)	−7.94789372(−5)	8	−4.39077230(−8)	1.66539324(−8)
4	−5.13184520(−5)	2.41268625(−5)			

[a]Read as $-3.73438354 \times 10^{+0}$.

TABLE 4. Coefficients $a_P^{(j)}$ and $a_T^{(j)}$ in (B 1) for $10^4 \leqslant k < 10^7$.

Then, in the same way as the estimate of A_1 in Chen *et al.* (2007), we have, by using (4.3*c*),

$$\left.\begin{aligned} \left|u\left[\psi_J^{(n)}\right]\right| &\leqslant C'[C_1 k^{-1}(\ln k+1)]^n \int_{-\infty}^{\infty}\int_{-\infty}^{\infty}\int_{0}^{\infty}\int_{-1/2}^{1/2} \frac{|\zeta_2|}{\zeta_1} \\ &\quad \times \exp\left(-\tfrac{\nu}{k|\zeta_1|}|s-x_1|\right) E^{1/2}\,\mathrm{d}s\,\mathrm{d}\zeta_1\,\mathrm{d}\zeta_2\,\mathrm{d}\zeta_3 \\ &\leqslant C''[C_1 k^{-1}(\ln k+1)]^n(\ln k+1), \end{aligned}\right\} \tag{A 9}$$

where C' and C'' are some positive constants. The estimate for $M[\psi_J^{(n)}]$ can be obtained in the same way.

Appendix B. Database of the net mass flows for the HS model

The database of the net mass flows for $k \geqslant 10$ that has been constructed in the present work makes use of the Chebyshev polynomial interpolation (see Boyd 2001) for $10 \leqslant k < 10^7$:

$$M[\phi_J] = \sum_{j=0}^{N} a_J^{(j)} P^{(j)}\left(\frac{\ln(k^2/(k_{max}k_{min}))}{\ln(k_{max}/k_{min})}\right), \tag{B 1}$$

where $P^{(j)}$ is the following polynomial of degree j of its argument:

$$P^{(0)}(x) = 1, \quad P^{(1)}(x) = x, \quad P^{(n)}(x) = 2xP^{(n-1)}(x) - P^{(n-2)}(x), \tag{B 2}$$

for $n \geqslant 2$ and $-1 \leqslant x \leqslant 1$, $(N, k_{min}, k_{max}) = (16, 10, 10^4)$ for $10 \leqslant k < 10^4$ and $(N, k_{min}, k_{max}) = (8, 10^4, 10^7)$ for $10^4 \leqslant k < 10^7$. The coefficients $a_J^{(j)}$ have been

determined by the numerical data of $M[\phi_J]$ computed for $N+1$ different values of k, say $k^{(l)}$, such that $\ln(k^{(l)2}/(k_{max}k_{min}))/\ln(k_{max}/k_{min}) = -\cos((2l+1)\pi/(2N+2))$ $(l = 0, \ldots, N)$. They are shown in tables 3 and 4. For economy of computation, the values of $a_T^{(j)}$ in the tables have been determined from the heat flow of the Poiseuille flow by using relation (6.4). (Note that the data of $M[\phi_T^{(i)}]$ and $M[\phi_P^{(i)}]$ $(i = 0, 1, n)$ in table 1 have been computed independently of each other.)

For $k \geqslant 10^7$, the database makes use of the first three terms of (6.1*a*):

$$M[\phi_J] = C_{J0} \ln k + C_{J1} + C_J[\nu], \tag{B 3}$$

where C_{J0} and C_{J1} are those in (6.1*b*) and $C_J[\nu]$ that for the HS model in table 2.

Appendix C. Grad's hard potential

In general, the collision frequency ν is written as

$$\nu(|\boldsymbol{\zeta}|) = 2\pi \int \int_0^{\pi/2} B(\theta, |\boldsymbol{\zeta}_* - \boldsymbol{\zeta}|) E(|\boldsymbol{\zeta}_*|)\, \mathrm{d}\theta\, \mathrm{d}\boldsymbol{\zeta}_*. \tag{C 1}$$

The hard potential introduced by Grad (1963) (Grad's hard potential) is defined as the potential satisfying the condition that

$$\frac{B(\theta, V)}{|\cos\theta \sin\theta|} < C(V + V^{-1+\epsilon}), \quad B_0(V) \geqslant C\frac{V}{1+V}, \tag{C 2}$$

where C and $\epsilon < 1$ are positive constants and

$$B_0(V) = \int_0^{\pi/2} B(\theta, V)\, \mathrm{d}\theta. \tag{C 3}$$

For Grad's hard potential, Grad (1963) showed that there are positive constants ν_0 and ν_1 such that $\nu_1(1+|\boldsymbol{\zeta}|^2)^{1/2} \geqslant \nu(|\boldsymbol{\zeta}|) \geqslant \nu_0 > 0$, that $\nu(|\boldsymbol{\zeta}|)$ is a monotonic increasing function of $|\boldsymbol{\zeta}|$ and that $\hat{K}$ defined by $\hat{K}(\hat{\phi}) = K(\phi)E^{1/2}$ with $\hat{\phi} = \phi E^{1/2}$ is a compact operator on L^2.

REFERENCES

Andries, P., LeTallec, P., Perlat, J. P. & Perthame, B. 2000 The Gaussian–BGK model of Boltzmann equation with small Prandtl number. *Eur. J. Mech.* B *Fluids* **19**, 813–830.

Bhatnagar, P. L., Gross, E. P. & Krook, M. 1954 A model for collision processes in gases. Part I. Small amplitude processes in charged and neutral one-component systems. *Phys. Rev.* **94**, 511–525.

Bird, G. A. 1994 *Molecular Gas Dynamics and the Direct Simulation of Gas Flows*. Oxford University Press.

Boyd, J. P. 2001 *Chebyshev and Fourier Spectral Methods*, 2nd (rev.) edn. Dover.

Cercignani, C. 1963 Plane Poiseuille flow and Knudsen minimum effect. In *Rarefied Gas Dynamics* (ed. J. A. Laurmann), vol. II, pp. 92–101. Academic.

Cercignani, C. 1988 *The Boltzmann Equation and its Applications*. Springer.

Cercignani, C. 2006 *Slow Rarefied Flows*. Birkhäuser.

Cercignani, C. & Sernagiotto, F. 1966 Cylindrical Poiseuille flow of a rarefied gas. *Phys. Fluids* **9**, 40–44.

Chen, C.-C., Chen, I.-K., Liu, T.-P. & Sone, Y. 2007 Thermal transpiration for the linearized Boltzmann equation. *Commun. Pure Appl. Math.* **60**, 0147–0163.

Grad, H. 1963 Asymptotic theory of the Boltzmann equation. Part II. In *Rarefied Gas Dynamics* (ed. J. A. Laurmann), vol. I, pp. 26–59. Academic.

Holway, L. H. Jr 1963 Approximation procedures for kinetic theory. PhD thesis, Harvard University, Cambridge, MA.

Holway, L. H. Jr 1966 New statistical models for kinetic theory: methods of construction. *Phys. Fluids* **9**, 1658–1673.

Kennard, E. H. 1938 *Kinetic Theory of Gases*. McGraw-Hill.

Kosuge, S., Sato, K., Takata, S. & Aoki, K. 2005 Flows of a binary mixture of rarefied gases between two parallel plates. In *Rarefied Gas Dynamics* (ed. M. Capitelli), pp. 150–155. AIP.

Kosuge, S. & Takata, S. 2008 Database for flows of binary gas mixtures through a plane microchannel. *Eur. J. Mech.* B *Fluids* **27**, 444–465.

Koura, K. & Matsumoto, H. 1991 Variable soft sphere molecular model for inverse-power-law or Lennard–Jones potential. *Phys. Fluids* A **3**, 2459–2465.

Loyalka, S. K. 1971 Kinetic theory of thermal transpiration and mechanocaloric effect. Part I. *J. Chem. Phys.* **55**, 4497–4503.

McCormack, F. J. 1973 Construction of linearized kinetic models for gaseous mixtures and molecular gases. *Phys. Fluids* **16**, 2095–2105.

Mori, M. 2005 Discovery of the double exponential transformation and its developments. *Publ. RIMS Kyoto Univ.* **41**, 897–935.

Mori, M. & Sugihara, M. 2001 The double-exponential transformation in numerical analysis. *J. Comput. Appl. Math.* **127**, 287–296.

Niimi, H. 1968 Thermal creep flow of rarefied gas through a cylindrical tube. *J. Phys. Soc. Japan* **24**, 225.

Niimi, H. 1971 Thermal creep flow of rarefied gas between two parallel plates. *J. Phys. Soc. Japan* **30**, 572–574.

Ohwada, T., Sone, Y. & Aoki, K. 1989 Numerical analysis of the Poiseuille and thermal transpiration flows between two parallel plates on the basis of the Boltzmann equation for hard-sphere molecules. *Phys. Fluids* A **1**, 2042–2049.

Sone, Y. 1969 Asymptotic theory of flow of rarefied gas over a smooth boundary. Part I. In *Rarefied Gas Dynamics* (ed. L. Trilling & H. Y. Wachman), vol. I, pp. 243–253. Academic.

Sone, Y. 1991 Asymptotic theory of a steady flow of a rarefied gas past bodies for small Knudsen numbers. In *Advances in Kinetic Theory and Continuum Mechanics* (ed. R. Gatignol & Soubbaramayer), pp. 19–31. Springer.

Sone, Y. 2007 *Molecular Gas Dynamics*. Birkhäuser. Supplemental notes and errata are available at: http://hdl.handle.net/2433/66098.

Sone, Y., Ohwada, T. & Aoki, K. 1989 Temperature jump and Knudsen layer in a rarefied gas over a plane wall: numerical analysis of the linearized Boltzmann equation for hard-sphere molecules. *Phys. Fluids* A **1**, 363–370.

Takahasi, H. & Mori, M. 1974 Double exponential formulas for numerical integration. *Publ. RIMS Kyoto Univ.* **9**, 721–741.

Takata, S. 2009 Symmetry of the linearized Boltzmann equation and its application. *J. Stat. Phys.* **136**, 751–784. ($(5/2)\gamma_2$ on line 18, p. 762, and line 24, p. 763, in this reference is a misprint of $(5/4)\gamma_2$.)

Welander, P. 1954 On the temperature jump in a rarefied gas. *Ark. Fys.* **7**, 507–553.